Bull. Mater. Sci. (2023) 46:48
https://doi.org/10.1007/s12034-022-02885-0

Novel MgO/few-layer graphene-filled polyaniline ternary nanocomposite as efficient electrode material in aqueous supercapacitors

DINESH BEJJANKI[1], SAMPATH KUMAR PUTTAPATI[1,*], HARITA PANT[2] and VADALI V S S SRIKANTH[2]

[1]Department of Chemical Engineering, National Institute of Technology, Warangal 506004, India
[2]School of Engineering Sciences and Technology, University of Hyderabad, Hyderabad 500046, India
*Author for correspondence (pskr@nitw.ac.in)

MS received 7 August 2022; accepted 4 November 2022

Abstract. MgO/few-layer graphene (FLG) nanocomposite is proven as an excellent electrode in aqueous supercapacitors (AS). The synergy between the pseudo-capacitive MgO and the double-layer charging nature of FLG that enhances the supercapacitors' specific capacitance (SC) was successfully tested. The SC could be further enhanced by combining MgO/FLG with a third component, such as a conducting polymer (with a Faradaic type of charge storage capability). Herein, such an attempt has been made. MgO/FLG was uniformly filled in polyaniline (PANI) by using a simple *in situ* polymerization method. X-ray diffraction, electron microscopy, and Raman and Fourier transform infrared spectroscopic analyses clearly showed the formation of a ternary nanocomposite constituted by MgO, FLG and PANI. As anticipated, the ternary nanocomposite (MgO/FLG-filled PANI (MFP)) exhibited an enhanced SC (compared to MgO/FLG) when tested as electrode material in AS. The MFP composite was evaluated for SC using a 3-electrode system. MFP composite exhibited a maximum SC of 347 F g^{-1} when tested at a scan rate of 5 mV s^{-1} using 1 M aqueous H_2SO_4 as the electrolyte. The electrode material assumable with symmetric capacitance achieved a maximum capacitance of 396 F g^{-1} at a current density of 1 A g^{-1} and showed a capacitance retention of 81%. In contrast, MgO/FLG exhibited much lower values under similar testing conditions.

Keywords. Nanocomposites; polymeric composites; energy storage and conversion.

1. Introduction

Recently, MgO/few-layer graphene (FLG; note: FLG is also known as reduced graphene oxide) (MF) nanocomposite has been demonstrated as an excellent dielectric material [1] and suitable electrode material for aqueous supercapacitors (AS) [2,3]. Other MgO-containing materials have also been shown as appropriate electrode materials for AS [4–8]. MgO is a naturally abundant, low-cost and low-toxic pseudo-capacitive material with a wide-operational potential range. Therefore, it has been chosen as one of the constituents in the electrode materials for AS. In the case of MF nanocomposites [1–3], MgO not only prevented the graphenaceous constituent's re-stacking, but its presence during synthesis also helped enhance the graphitic nature of the graphenaceous component. The synergy between the pseudo-capacitive MgO and the double-layer charging nature of FLG to enhance the supercapacitors' specific capacitance (SC) was also successfully tested [3]. MF nanocomposite exhibited excellent cyclic stability (95% of discharge capacitance was retained even after the 5000th cycle). It is now hypothesized that the SC could be further enhanced by combining MgO/FLG with a third component, such as a conducting polymer (with a Faradaic type of charge storage capability). Therefore, this work has been planned to prepare a ternary nanocomposite constituted by MgO, FLG and polyaniline (PANI), and test it as electrode material in AS. It should be noted that PANI nanostructures [9,10] and carbon-filled PANI nanocomposites [11,12] are well-tested electrode materials (with attractive SC values and excellent cyclic stability) for AS. Therefore, the proposed MgO/FLG-filled PANI (MFP) ternary nanocomposite can be considered a new addition to the list of (i) safe, (ii) easily processable, (iii) easily applicable (in the form of paint, solid cake, free-standing film) and (iv) high-performing electrode materials for AS.

2. Experimental

2.1 *Material and methodology*

Synthesis and different characteristics of MgO/FLG are given in reference [3]. MFP ternary nanocomposite

Published online: 04 March 2023

preparation is as follows: Firstly, 250 ml of 1 M HCl was taken in a round bottom flask. Then, 20 ml of vacuum-distilled aniline was added to it. Subsequently, 1 wt% (relative to the amount of aniline monomer) of MgO/FLG nanocomposite powder was added to the reaction mixture, then ultrasonicated for 1 h to disperse MgO/FLG particles in the aniline monomer uniformly. Next, the reaction mixture was cooled to 0°C using an ice bath. The polymerization was then initiated by rapidly adding ammonium persulphate (APS) (in 1:4 molar ratio with respect to aniline) to the reaction mixture (i.e., HCl + aniline + MgO/FLG nanocomposite). During APS addition, the reaction mixture's temperature was maintained in the range of 0–5°C. After APS addition, the reaction mixture was left stirring for 4 h to form a dark green-coloured wet cake, which was finally dried at 90°C under vacuum for 48 h to obtain MFP nanocomposite as revealed by the characterization methods.

2.2 *Characterization*

X-ray diffraction (XRD) was carried out to understand the crystallinity of MFP nanocomposite. XRD pattern was recorded using Cu Kα as the X-ray source ($\lambda = 1.54$ Å); Bruker's AXS Model D8 Advance System was used to record the XRD pattern. Field emission scanning electron microscope (FESEM, Zeiss Ultra 55) with an operating voltage of 5 kV was used to record the morphology of MFP nanocomposite. Transmission electron microscope (TEM, FEI Technai G2 S-Twin) with an operating voltage of 200 kV was used to record the morphology and crystallinity of MFP nanocomposite. Raman scattering was carried out to obtain the phase information of MFP nanocomposite. Raman spectrum was recorded with a spectral resolution of 1 cm^{-1} using 514.5 nm Ar^{+} ion laser (LabRam HR800 Raman spectrometer). Fourier transform infrared (FTIR) spectroscopy was carried out using a board IR light to complement the Raman analysis.

CHI660D CHI electrochemical workstation was used for electrochemical measurements at room temperature in a three-electrode configuration with the MFP nanocomposite-coated Ni foam as the working electrode, Hg/HgO (saturated) as the reference electrode, and Pt ring as the counter electrode in 1 M H_2SO_4 electrolyte solution. Active electrode material slurry was made through a standard procedure, i.e., by mixing 80 mg of MFP nanocomposite, 10 mg of super p carbon black, and 10 mg of polyvinylidene fluoride binder (in the mass ratio 80:10:10) in 10 ml of *N*-methyl-2-pyrrolidone (NMP). The slurry was then drop-casted on the surface of the Ni foam, which was kept in a vacuum oven for 6 h to allow the evaporation of the NMP. Cyclic voltammetry (CV) studies are carried out at different scan rates of 5, 10, 20, 30, 50 and 100 mV s^{-1}. Galvanostatic charge–discharge (GCD) cycling was carried out at different current densities (0.5, 1, 2, 5 and 10 A g^{-1}) in the potential range of −0.2 to 1 V. For the three-electrode system, the SC, energy density (ED) and power density (PD) are calculated using the following standard formulae:

$$\mathrm{SC} = \frac{A}{m \times \Delta V \times k}$$

$$\mathrm{ED} = \frac{1}{2} \times \mathrm{SC} \times (\Delta V)^2$$

$$\mathrm{PD} = \frac{\mathrm{ED}}{\Delta t}$$

where A is the area enclosed under the curve, m the mass loading, ΔV the potential window difference, k the scan rate and Δt the discharge time.

3. Results and discussion

3.1 *Morphology and structure analysis*

The XRD pattern of MFP nanocomposite is shown in figure 1. The peaks centred at 2θ=20.4° and 25.7° are attributed to periodicity parallel and perpendicular to the polymer chain in PANI, respectively. However, the peak at 2θ=25.7° is broad, indicating that it is a result of the convolution of the diffraction peak (typically appearing at $2\theta = \sim 26°$) corresponding to (002) FLG and the diffraction peak corresponding to (110) PANI in electrically conducting emeraldine salt form. (110) PANI peak should typically appear at 2θ=26°, but the observed shift (now appearing at 2θ=25.7°) is an indication of the formation of PANI nanofibres [9,11] on the surfaces of FLG particles. The diffraction signal observed at $2\theta = \sim 43°$ is due to the combination of (100) MgO diffraction signal and (200) graphite-like diffraction signal from the walls of FLG. The XRD observations are consistent with those reported for MF [3] and PANI nanocomposites, indicating the formation of MFP nanocomposite. FESEM images of MFP nanocomposite are shown in figure 2. In these images, it is observed

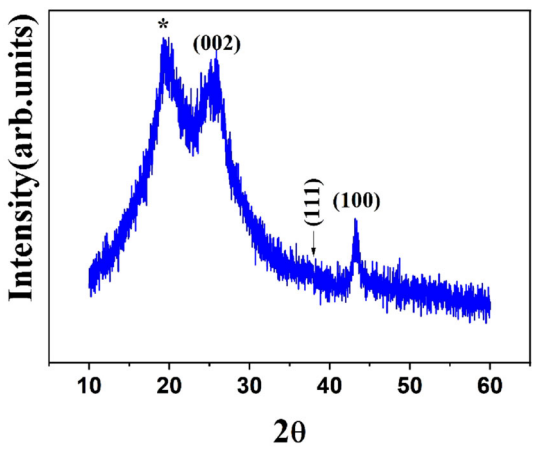

Figure 1. X-ray diffractogram of the MFP nanocomposite.

that PANI nanofibres are nicely coated on the MgO/FLG particles. Figure 3 shows the TEM image of MgO/FLG–PANI nanocomposite. From the micrographs it is seen that the polyaniline is nicely coated on the MgO (cube shape), which is not seen in figure 1. Selected area electron diffraction pattern shown in figure 3b indicates semi-crystallinity of the sample owing to the presence of polyaniline.

3.2 *Bonding analysis using Raman spectroscopy and FTIR*

The Raman spectrum of the MFP nanocomposite is shown in figure 4. The spectrum contains three Raman bands at ~1355, ~1568 and ~2870 cm^{-1} corresponding to the combination of protonated imine form of PANI, i.e., C–N^+ de-localized polaronic structure and D band in FLG [10], C–C stretching of benzenoid ring of PANI and G band in FLG, and 2D band in FLG [11]. The Raman observations confirm that the as-prepared MFP nanocomposite is constituted by both PANI and FLG [12]. However, in the present case, due to the strong overlap of Raman signals, the FLG and PANI Raman bands could not be separately identified [13–15]. The typical PANI bands at ~1497, ~1566and ~1618 cm^{-1} correspond to C–N of the benzene diamine units, C–C plus C–N stretching, C=C of the quinoid rings and C–C of the benzenoid rings, respectively, in PANI. These bands have overlapped with the typical D and G bands of FLG. However, FTIR spectroscopic analysis was useful in identifying different functional groups in the MFP nanocomposite. The FTIR spectrum of the MFP nanocomposite is shown in figure 5. The band at ~495 cm^{-1} is attributed to the absorption related to Mg–O bond vibrations, and the bands at ~1560 and ~1485 cm^{-1} are attributed to the absorption related to stretching vibrations between C=N (quinoid ring) and C=C (benzenoid ring) of PANI. The bands at ~1235 and ~1295 cm^{-1} correspond to the absorption related to vibrations of the C–N bond with an aromatic conjugation. The typical band at ~3415 cm^{-1} is assigned to –OH stretching mode, while the bands at ~1570 and 615 cm^{-1} are attributed to the absorption related to C=C stretching in FLG and C–N–C bond, indicating the presence of aromatic rings in the MFP nanocomposite. All in all, Raman and FTIR spectroscopic analyses confirm the presence of MgO, PANI and FLG in the MFP nanocomposite. The analysis also indicates that the constituents have appropriate bonding structures that enable them to store charge [6,11].

3.3 *Electrochemical measurements*

CV curve of MFP nanocomposite at a scan rate of 5 mV s^{-1} is shown in figure 6a, while the CV curves at various scan rates are shown in figure 6b. It is clear from the typical shape of the CV curves that they are a result of both pseudo-capacitance (due to PANI and MgO) and electrical double-layer capacitance (EDLC; due to FLG) components corresponding to the presence of respective constituents in the nanocomposite. The functionalization of MgO–FLG with PANI results in high current and more enclosed area. The redox peak couples shown in figure 6a, first (C1/A1) at ~0.2 V correspond to the transition of PANI between a leuco emeraldine to polaronic emeraldine form, and the second (C2/A2) at ~0.45 V corresponds to the transition of PANI between a polaronic emeraldine to pernigraniline form [11,12,16]. It is clear from the typical shape of the CV curves that they are a result of both pseudo-capacitance (due to PANI and MgO) and EDLC (due to FLG) components corresponding to the presence of respective constituents in the nanocomposite. Due to the domination of PANI and FLG peaks in CV curves, the MgO peaks are not discernable. It is observed that with an increase in scan rates, there is a shift in redox peaks, which is indicative of good ion response (EDLC behaviour). Also, high currents (with an increase in scan rates) in the CV curves indicate low internal resistance of the MFP nanocomposite. Figure 6c shows the SC values of the MFP nanocomposite at various scan rates. At the scan rate of 5 mV s^{-1}, the MFP nanocomposite exhibited a maximum SC of 347 F g^{-1}. It

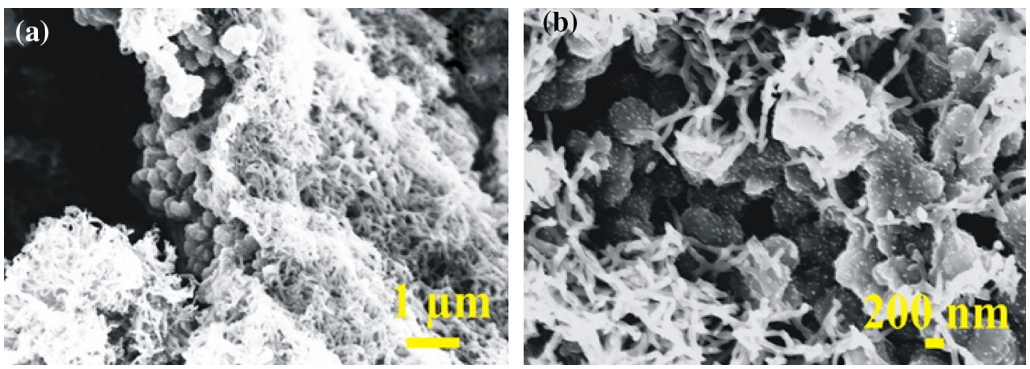

Figure 2. (**a**) Low- and (**b**) high-magnification scanning electron micrographs of the MFP nanocomposite, respectively.

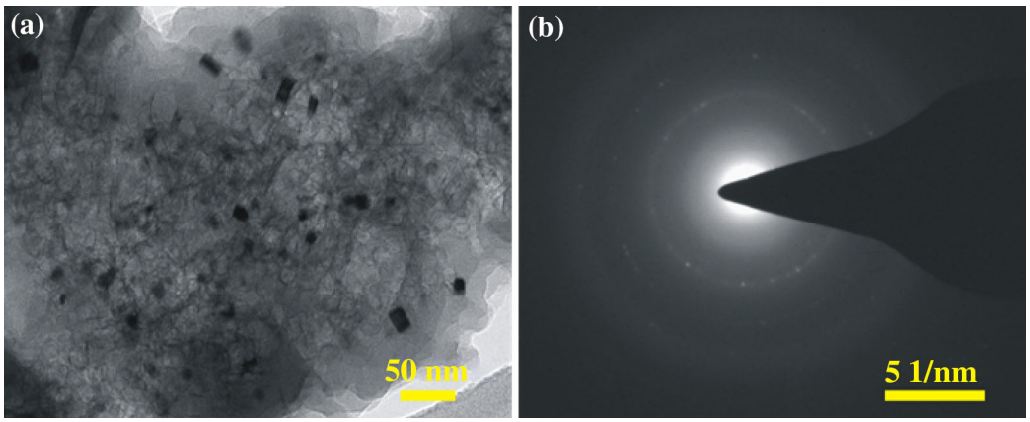

Figure 3. (**a**) TEM image and (**b**) the corresponding diffraction pattern of the MFP nanocomposite.

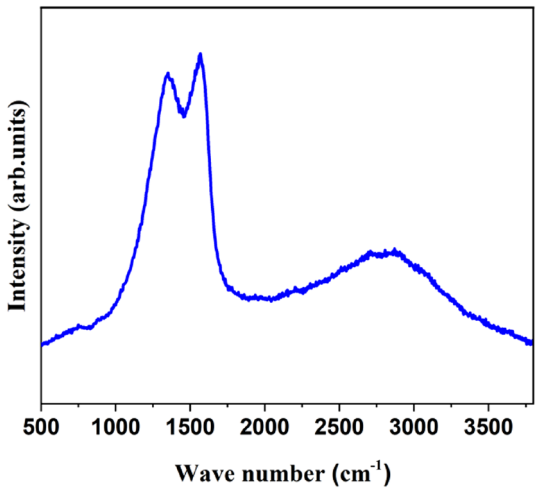

Figure 4. Raman spectrum of the MFP nanocomposite.

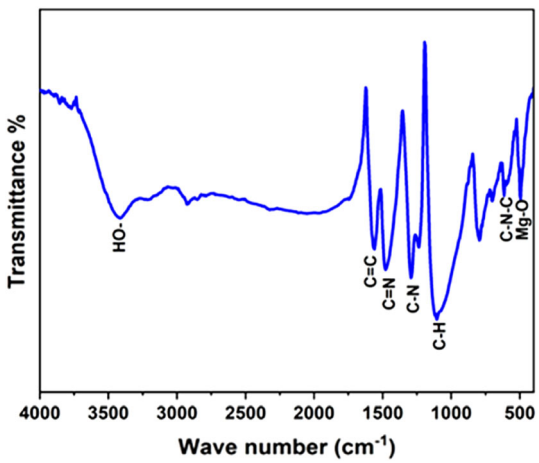

Figure 5. FTIR spectrum of the MFP nanocomposite.

may be noted that MF nanocomposite exhibited SC values less than 180 F g^{-1} under similar testing conditions. Even at a scan rate of 10 mV s^{-1}, the MFP nanocomposite outperformed the MF nanocomposite. The enhanced SC values in the case of MFP nanocomposite are attributed to the efficient charge transfer and consequently improved the electrochemical performance due to the large-scale π–π conjugation between PANI and FLG constituents in MFP nanocomposite as revealed by complementary characterization techniques. The typical triangular shape of GCD curves recorded at various current densities (figure 6d) indicates the redox nature of the constituents (in this case, MgO and PANI) of MFP nanocomposite. These curves also show a considerable increase in the discharge time in the case of MFP nanocomposite compared to MF nanocomposite [3]. At 0.5 A g^{-1}, the MFP nanocomposite exhibited an ED of 199.03 Wh kg^{-1} and a PD of 1380 W kg^{-1}. The PD and ED are 97.6 Wh kh^{-1} and 3600 W kg^{-1}, respectively, when measured in the two-electrode configuration. On the contrary, MF composite delivered a specific capacitance of only 168 F g^{-1} at 0.5 A g^{-1} [3]. Similarly, the MFP composite was operated for 1000 cycles, as show in figure 6e, with a good capacitance of 396 F g^{-1} and a capacity retention of 81%, implying a definite enhancement in energy storage capacitance due to the preparation of the MFP nanocomposite. Electrochemical impedance spectroscopy measurement was carried out to study the behaviours of electrodes. The Nyquist plot for MFP in 1 M H_2SO_4 at a potential of 0.5 V and frequency range of 0.01 Hz to 10 kHz is shown in figure 6f. The plot consists of an intercept on the *X*-axis with solution resistance R_s of 2.281 Ω and charge transfer resistance R_{ct} of 0.001 Ω, followed by a straight line with making an angle of 45° with ion diffusion resistance or Warburg resistance of 0.01108 Ω. The graph shows less resistance thereby resulting in a better performance in two-electrode system. Further, from electrochemical impedance spectroscopy analysis, SC was calculated using standard formula $SC=4(-(1/2\pi f Z'' m))$, where m is mass of MFP electrode material (g), f is frequency in Hz and Z'' is imaginary value. The MFP composite from Nyquist plot showed capacitance of 316 F g^{-1}, which is almost similar to the stable SC from charge–discharge graph.

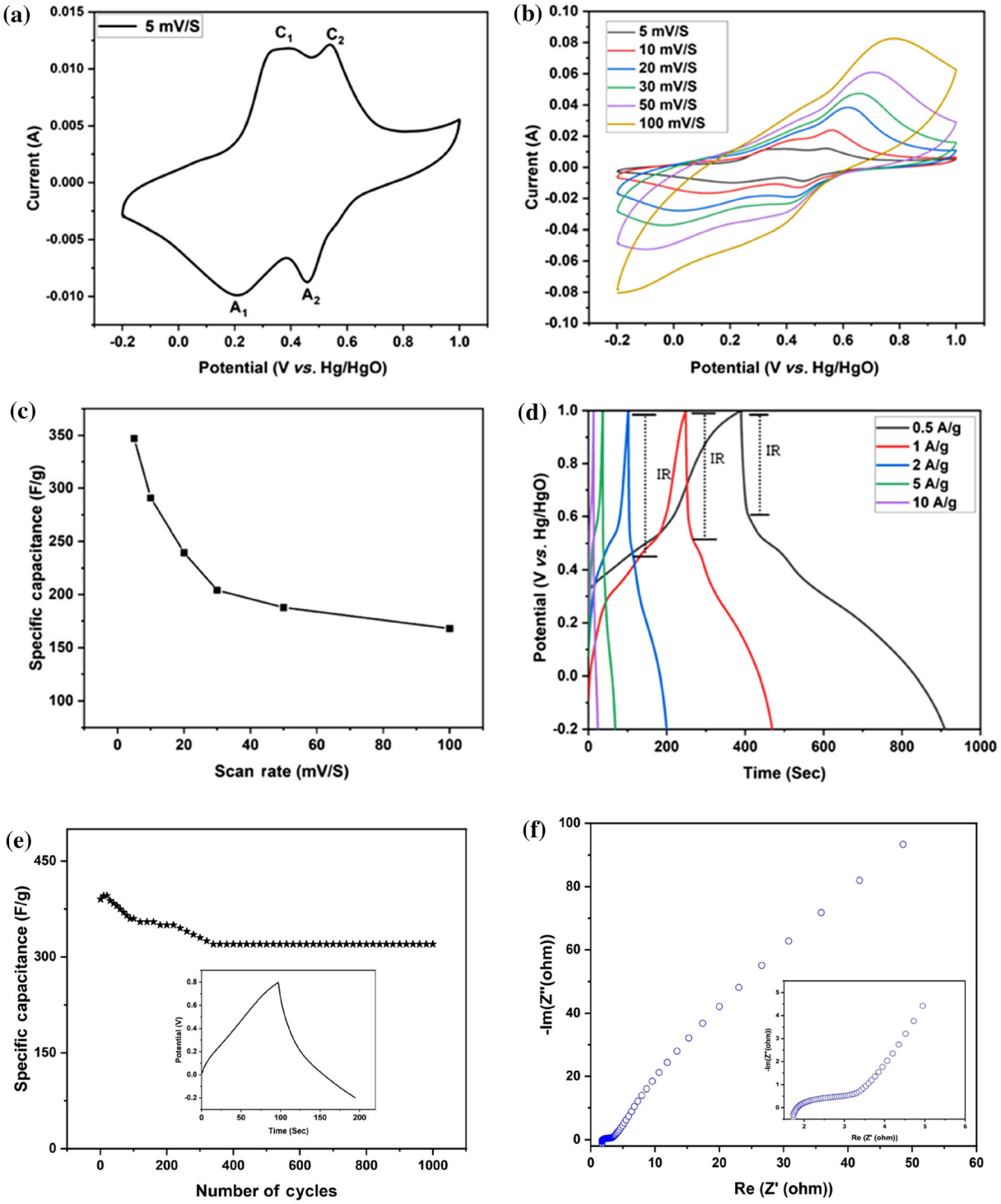

Figure 6. (**a**) CV curve at 5 mV s^{-1} scan rate, (**b**) CV curves at various scan rates, (**c**) specific capacitance values *vs.* scan rate, and (**d**) GCD curves at a current density of 1 A g^{-1} of the MFP nanocomposite. (**e**) Charge–discharge curve of MFP composite using two-electrode system and (**f**) electrochemical impedance spectroscopy presented as Nyquist graph for MFP composite.

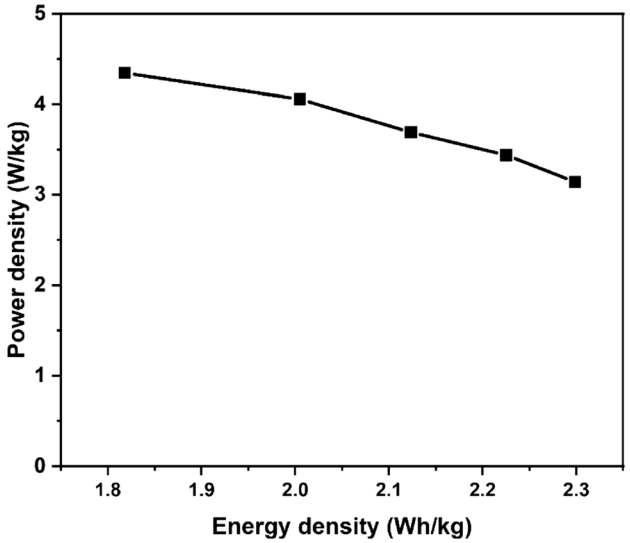

Figure 7. Ragone plot of the MFP nanocomposite.

4. Conclusions

By preparing a ternary nanocomposite constituted by MgO, FLG and PANI, the SC was considerably enhanced compared to a nanocomposite constituted by only MgO and FLG. The redox nature of PANI has helped in the enhancement of SC values at different scan rates. The ternary nanocomposite exhibited SC of 347 F g^{-1} at a scan rate of 10 mV s^{-1} as well as energy and power densities of 199.03 Wh kg^{-1} and 1380 W kg^{-1} at a current density of 0.5 A g^{-1}, respectively, and the composite showed good cyclic stability with 81% capacitance retention, which attributed to the observed synergy between the redox contributions from MgO and PANI as well as the EDLC contribution from FLG. The Ragone plot of the nanocomposite is shown in figure 7.

Acknowledgement

VVSSS acknowledges financial support to UoH-IoE by MHRD (F11/9/2019-U3(A)).

References

[1] Jammula R K and Srikanth V V S S 2017 *Diam. Relat. Mater.* **80** 18
[2] Das P S, Bakuli S, Biswas I, Mallik A K, Dey A, Mukherjee S *et al* 2018 *Ceram. Int.* **44** 424
[3] Petnikota S, Srikanth V V S S, Toh J J, Srinivasan M, Bobba C V R, Adams S *et al* 2019 *New J. Chem.* **43** 9793
[4] Karthikeyan K, Amaresh S, Aravindan V and Lee Y S 2013 *J. Mater. Chem. A* **1** 4105
[5] Marimuthu M, Ganesan S and Johnbosco J Y 2020 *Electrochim. Acta* **357** 136848
[6] Gedela V R and Srikanth V V S S 2014 *Appl. Phys. A: Mater. Sci.* **115** 189
[7] Eftekhari A, Li L and Yang Y 2017 *J. Power Sources* **347** 86
[8] Gedela V, Puttapati S K, Nagavolu C and Srikanth V V S S 2015 *Mater. Lett.* **152** 177
[9] Wang X, Wu D, Song X, Du W, Zhao X and Zhang D 2019 *Molecules* **24** 12
[10] Iqbal J, Ansari M O, Numan A, Wageh S, Al-Ghamdi A, Alam M G *et al* 2020 *Polymers* **12** 12
[11] Petnikota S, Rotte N K, Reddy M V, Srikanth V V S S and Chowdari B V R 2015 *ACS Appl. Mater. Interfaces* **7** 2301
[12] Gholami Laelabadi K, Moradian R and Manouchehri I 2020 *ACS Appl. Energy Mater.* **3** 5301
[13] Morajkar P P, Abdrabou M K, Salkar A V, Raj A, Elkadi M and Anjum D H 2020 *Energy Fuels* **34** 12960
[14] Da Costa S, Salkar A, Krishnasamy A, Fernandes R and Morajkar P 2022 *Fuel* **309** 122141
[15] Hsiao Y S, Chang Jian C W, Huang T Y, Chen Y L, Huang J H, Wu N J *et al* 2022 *J. Taiwan Inst. Chem. Eng.* **134** 104318
[16] Lv P, Tang X, Zheng R, Ma X, Yu K and Wei W 2017 *Nanoscale Res. Lett.* **12** 630